Skin Model Surface Temperatures During Single and Multiple Cryogen Spurts Used in Laser Dermatologic Surgery

Julio C. Ramirez-San-Juan, PhD,[1,2] Guillermo Aguilar, PhD,[1,3]* Alia T. Tuqan,[1] Kristen M. Kelly, MD,[1,4] and J. Stuart Nelson, MD, PhD[1,4]

[1]*Beckman Laser Institute and Medical Clinic, University of California, Irvine, California 92612*
[2]*Departamento de Optica, INAOE, AP 51 y 216, CP 72000 Puebla, Pue., Mexico*
[3]*Department of Mechanical Engineering, University of California, Riverside, California 92521*
[4]*Department of Dermatology, University of California, Irvine, California 92612*

Background: Although cryogen spray cooling (CSC) is used to minimize the risk of epidermal damage during laser dermatologic surgery, concern has been expressed that CSC may induce cryo-injury. In order to address this concern, it is necessary to evaluate the effects of prolonged exposure of human skin phantoms (HSP) to CSC.

Objective: To measure the minimum surface temperature (T_{min}) and the time at which it occurs (t_{Tmin}) as well as determine the time the sprayed HSP surface remains below 0°C (sub-zero time, Δt_s) and −26°C (residence time, Δt_r) during the application of single (SCS) and multiple (MCS) cryogen spurts. Two initial HSP substrate temperatures were studied, T_i: 23 and 70°C.

Study Design/Materials and Methods: An epoxy-based HSP was constructed to measure T_{min}, t_{Tmin}, Δt_s, and Δt_r, for 17 spray patterns: 1 SCS with a total cryo-delivery time (Δt_c) of 40 milliseconds; 8 MCS patterns with identical Δt_c, but with a total cooling time (Δt_{total}) varying from 50 to 280 milliseconds; and 8 SCS patterns that matched the Δt_{total} of the MCS patterns.

Results: For both T_i, our results show that it is possible to distinguish between two different cooling regimes. For $\Delta t_{total} \leq 110$ milliseconds, the differences between SCS and MCS patterns with the same Δt_{total} for all variables (T_{min}, t_{Tmin}, Δt_s, Δt_r) are negligible. Most importantly, all these variables show a remarkable linear dependence with Δt_{total}. In the interval 110 milliseconds $< \Delta t_{total} <$ 280 milliseconds, T_{min} and t_{Tmin} are similar for SCS and MCS, while Δt_s and Δt_r show more pronounced differences between the two spray patterns. In this interval, the values of T_{min} and Δt_s for MCS remain invariant and similar to the corresponding values for $\Delta t_{total} = 110$ milliseconds.

Conclusions: These results suggest that: (1) similar epidermal protection may be attained with SCS and MCS for $\Delta t_{total} \leq 110$ milliseconds; and (2) for 110 milliseconds $< \Delta t_{total} \leq 280$ milliseconds, MCS help to maintain Δt_s similar to that of SCS at $\Delta t_{total} = 100$ milliseconds, which may be beneficial to prevent cryo-injury. Lasers Surg. Med. 36:141–146, 2005. © 2005 Wiley-Liss, Inc.

Key words: dynamic cooling; cooling selectivity; cryo-injury; port wine stain

INTRODUCTION

The importance of cryogen spray cooling (CSC) in conjunction with laser therapy of various dermatoses such as port wine stain (PWS) [1,2], telangiectasias, hemangiomas [3], hair-removal, and rhytides [4] has been widely documented [5]. CSC prevents excessive heating of the superficial skin layers, thus allowing the safe use of higher light doses while avoiding complications such as hypertrophic scarring or dyspigmentation [6].

When compared to other epidermal cooling methods, CSC is particularly useful for treatment of superficial targeted lesions, since it permits [7]: (1) accurate control of the cryogen application time (typically 5–100 milliseconds) and, consequently, cooling time; and (2) high heat transfer rates as cryogen is deposited onto the skin and evaporates very quickly therefrom. These two characteristics are instrumental in achieving efficient and spatially selective epidermal cooling.

Despite these advantages, concern has been expressed that CSC may induce cryo-injury [8]. In order to address this concern, computational models [9], epoxy phantoms [7,10] and, more recently, human skin tissue culture models (RAFT) [11] have been used to evaluate the effects of prolonged exposure of human skin to CSC.

Contract grant sponsor: National Institutes of Health (to G.A.); Contract grant number: HD42057; Contract grant sponsor: Dermatology Foundation and the American Society for Laser Medicine and Surgery (to K.M.K.); Contract grant sponsor: National Institutes of Health (to J.S.N.); Contract grant numbers: GM62177, AR48458, AR47551.

*Correspondence to: Guillermo Aguilar, PhD, Department of Mechanical Engineering, University of California, Riverside CA 92521. E-mail: gaguilar@engr.ucr.edu

Accepted 5 November 2004
Published online 21 February 2005 in Wiley InterScience (www.interscience.wiley.com).
DOI 10.1002/lsm.20124

In this work, we investigate systematically the thermal response of human skin phantoms (HSP) by measuring the minimum surface temperature (T_{min}) and the time (t_{Tmin}) at which it occurs, as well as determine the time the sprayed surface remains below 0°C (sub-zero time, Δt_s) and −26°C (residence time, Δt_r) during the application of single (SCS) and multiple (MCS) cryogen spurts for two initial HSP substrate temperatures T_i: 23 and 70°C.

METHODS AND PROCEDURES

Numerical Simulation

We computed the radiant energy distribution resulting from a single laser pulse (beam radius = 5 mm; fluence = 4 J/cm^2) using the well-known Monte Carlo code (MCML/CONV) developed by Wang et al. [12,13]. In order to estimate the total heat extracted from the HSP surface throughout a specific cryogen-laser pattern, we developed a numerical simulation using commercial finite element software (FEMLAB^{TM}, COMSOL, Burlington, MA). The output of the Monte Carlo code is entered as the heat source required by the FEMLAB code [14] to simulate heat diffusion. For simplicity, each cryogen spurt was simulated by imposing a convective boundary condition on the HSP surface with constant h (heat transfer coefficient) and T_c (cryogen temperature) values of 7,000 W/m^2 K and −40°C, respectively.

We simulated a cryogen-laser pattern similar to those employed in commercially available devices, as represented in Figure 1. The thickness, thermal [9] and optical [15] properties of human skin layers used for calculations of the radiant energy distribution and total heat extracted, respectively, are shown in Table 1.

HSP

The HSP consisted of a thin (90 μm) rectangular (3.42×3.50 mm) silver foil placed on top of an epoxy resin and a type-K thermocouple of ~50 μm bead diameter with a response time of 3 milliseconds (Omega, Stamford CN), positioned in between. Thermal paste was applied around the bead to ensure good thermal contact. The foil was sufficiently thin to ensure fast response and a spatially averaged measurement. The purpose of the HSP was to provide thermal properties on the same order of magnitude as those of human skin [9,10]. In general, the CSC procedures are used clinically at room temperature, which is the reason for selecting T_i = 23°C; however, it is believed that 70°C is the threshold temperature for instantaneous skin-thermal injury [16]. Therefore, and in order to simulate heat generated by the laser pulses, in another series of experiments a copper plate heated (by a pair of thermo-electric coolers: TEC) the HSP to T_i of 70°C prior to cryogen application.

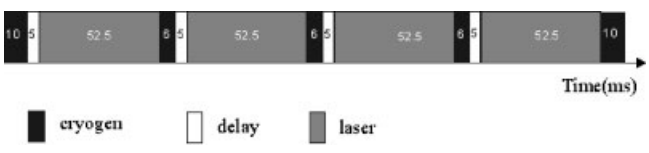

Fig. 1. Schematic showing alternate cryogen spray, delay time, and laser pulses employed in our numerical simulation.

TABLE 1. Thickness, Thermal and Optical Properties of Human Skin Layers Used With the Finite Element and MCML/CONV Models for λ = 1,450 nm

	Layer	
	Epidermis	Dermis
Thickness (mm)	0.05	1
k (W/(m K))	0.21	0.53
ρ (kg/m^3)	1,200	1,200
c (J/(kg K))	3,600	3,800
μ_a (1/cm)	20	2
μ_s (1/cm)	120	120
g	0.9	0.9
n	1.37	1.37

Cryogen Delivery

The only FDA-approved cryogen compound currently used in laser dermatologic surgery is 1,1,1,2 tetrafluoroethane, also known as R134a, with boiling temperature T_b ≈−26.2°C at atmospheric pressure. R-134a is contained at saturation pressure (6.7 bar at 25°C) and delivered through a standard high-pressure hose to a control valve. A commercial cryogen spray nozzle (with approximate inner diameter of 0.5 mm) used for laser treatment of vascular lesions and hair removal was employed to spray the cryogen on to the HSP.

The nozzle-to-sprayed surface distance, z, was 31 mm, (similar to that currently used in several commercially available CSC devices) for all experiments. The relative humidity was 39% and the room temperature ≈23°C. A schematic of the experimental setup is shown in Figure 2.

In this study, we employed electronically controlled SCS and MCS spray patterns. T_{min}, t_{Tmin}, Δt_s, and Δt_r, were systematically measured for 17 spray patterns: (a) 1 SCS of

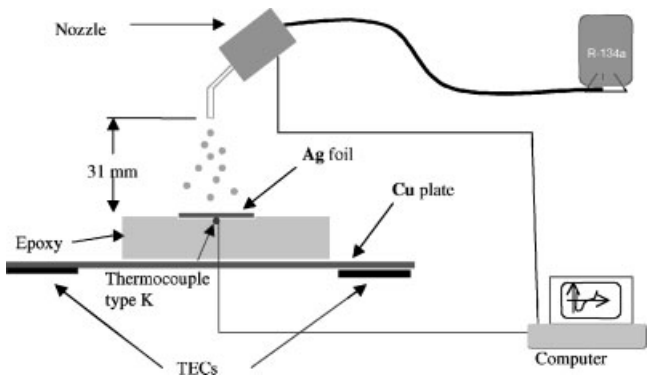

Fig. 2. Experimental system employed to measure the sprayed HSP surface temperatures during the application of SCS and MCS, for two different T_i HSP temperatures (23 and 70°C).

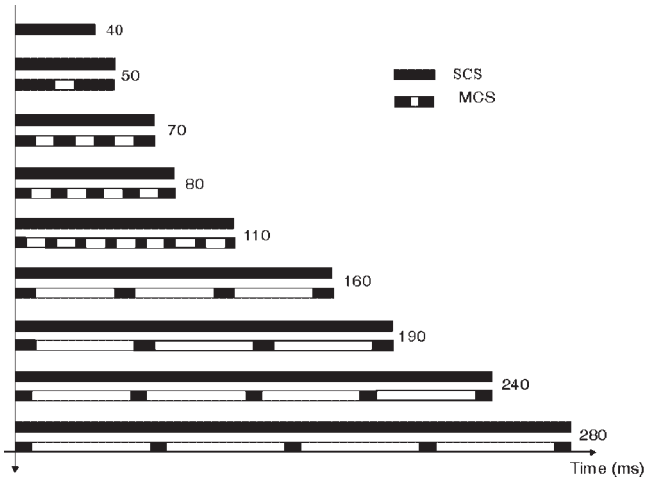

Fig. 3. SCS and MCS spray patterns under study. The asterisk denotes the spray patterns studied by Tuqan et al. [11].

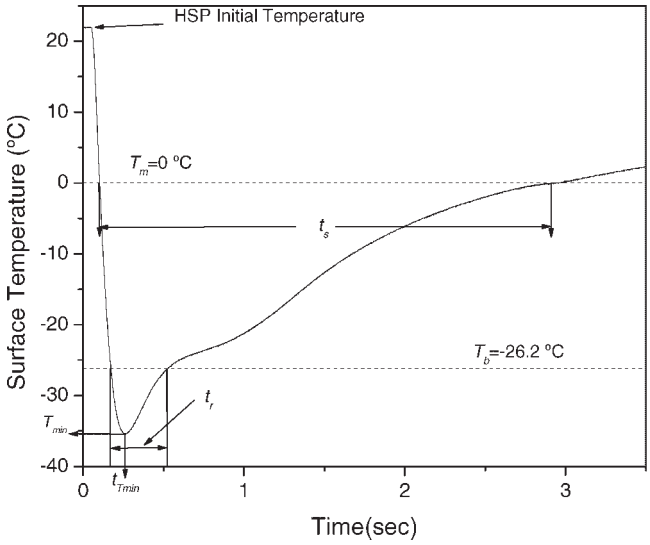

Fig. 4. Schematic of a typical temperature curve versus time for a MCS at a spray distance (z) = 31 mm. Characteristic features are minimum temperature ($T_{\min}$); time at which $T_{\min}$ is reached (t_{Tmin}); sub-zero time (Δt_s); liquid cryogen residence time (Δt_r); boiling point of R134a (T_b), and freezing point of water (T_m).

$\Delta t_c = 40$ milliseconds; (b) 8 MCS patterns with identical Δt_c of 40 milliseconds, but with a constant time interval between consecutive spurts, which resulted in a variation of the total cooling time ($\Delta t_{\mathrm{total}}$) from 50 to 280 milliseconds; and (c) 8 SCS patterns that matched the $\Delta t_{\mathrm{total}}$ of the MCS patterns described above. A schematic of the experimental spray patterns is shown in Figure 3.

RESULTS AND DISCUSSION

Although the dynamics of a MCS spray pattern of CSC and laser-induced heating is different from that of a SCS of same $\Delta t_{\mathrm{total}}$ followed by one laser pulse, both spray patterns can be compared in terms of the total heat extracted. According to the numerical simulation described above with the optical and thermal parameters described therein, the total heat extracted through the pattern shown in Figure 1 is ~10.9 kJ/m^2, which is similar to that (~9.2 kJ/m^2) from the pre-heated HSP (at 70°C) exposed to a SCS of 40 milliseconds. For this reason, the Δt_c for all MCS patterns was selected to be 40 milliseconds.

Figure 4 shows a typical HSP surface temperature measurement in response to a MCS pattern as well as the definitions employed to describe the temperature profile as a function of time. As spray droplets impinge on the surface, very fast heat extraction occurs at the cryogen–HSP interface. A rapid decrease in surface temperature (quantitatively similar to that expected to occur on human skin) is noted and continues for some time after spurt termination. A $T_{\min}$ is reached at a certain time (t_{Tmin}), which depends on the $\Delta t_{\mathrm{total}}$ employed in each cryogen spray pattern. Often, the interface can reach and maintain a local constant temperature near (T_b) for several milliseconds which may be attributed to the presence of a thin residual cryogen layer, which evaporates during and after spurt termination. Aguilar et al. [7] defined the Δt_r as the period that the surface temperature remains below (the cryogen boiling point) $T_b \approx -26.2$. The increase in temperature from T_b up to the freezing temperature of water (T_m) is gradual and relatively linear. Often, a plateau is noted at T_m, which may be attributed to condensation, freezing, and subsequent melting of ambient water on the surface. The period the surface temperature remains below 0°C is defined as the Δt_s. Water condensation and freezing on the sprayed surface do not occur during the spurt, despite the sub-zero temperature that may have been reached [17,18]. This is because tetrafluorethane is a hydrophobic compound, which impedes the mixing of cryogen with water and, therefore, does not allow frost to form on the sprayed surface until the cryogen has evaporated completely [7].

Figures 5 and 6 show, respectively, $T_{\min}$ and t_{Tmin} as a function of $\Delta t_{\mathrm{total}}$ for all spray patterns described in Figure 3 and for the two initial HSP temperatures, T_i (23 and 70°C). For $T_{\min}$, the differences between SCS and MCS with the same $\Delta t_{\mathrm{total}}$ are small. Note, however, that $T_{\min}$ has a strong dependence on T_i (between 12 and 18°C). For $T_i = 23$°C, $T_{\min}$ varies between −40 and −46°C (~15%) and, for $T_i = 70$°C, $T_{\min}$ varies between −20 and −32°C (~60%) for the range of $\Delta t_{\mathrm{total}}$ under study. From Figure 5, it is possible to distinguish between two different cooling regimes. For $\Delta t_{\mathrm{total}} \leq 110$ milliseconds, $T_{\min}$ shows a linear dependence with $\Delta t_{\mathrm{total}}$. In the interval 110 milliseconds $< \Delta t_{\mathrm{total}} \leq$ 280 milliseconds, $T_{\min}$ reaches an asymptotic value (−46°C for $T_i = 23$°C and −32°C for $T_i = 70$°C), for both SCS and MCS. Figure 6 also shows the linear dependence of t_{Tmin} with $\Delta t_{\mathrm{total}}$, although the same dependence holds throughout the entire range of $\Delta t_{\mathrm{total}}$. The slope of this linear behavior is ~1, which means that for both SCS and MCS, $T_{\min}$ is always reached at spurt termination for all parameters under study and there is no dependence on T_i.

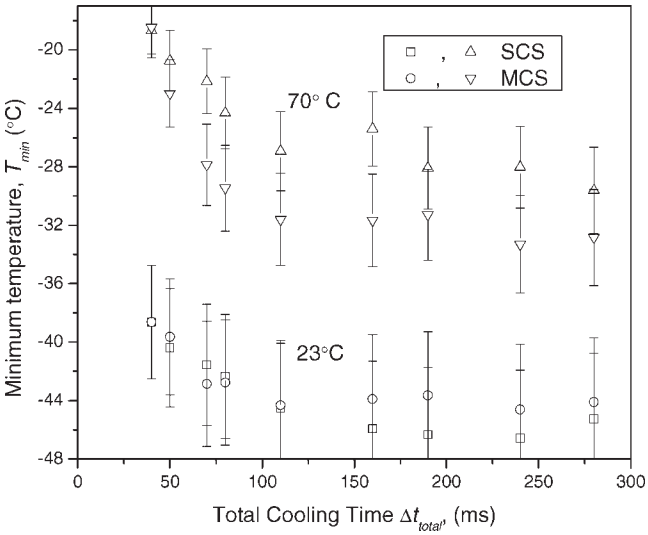

Fig. 5. Minimum surface temperature ($T_{\min}$) versus total cooling time (Δt_{total}) for SCS and MCS at two different T_{i} HSP temperatures. Two different cooling regimes are distinguished: For $\Delta t_{\text{total}} \leq 110$, $T_{\min}$ shows a linear decrease with the Δt_{total}, and for 110 milliseconds $< \Delta t_{\text{total}} \leq 280$ milliseconds, $T_{\min}$ is similar for SCS and MCS.

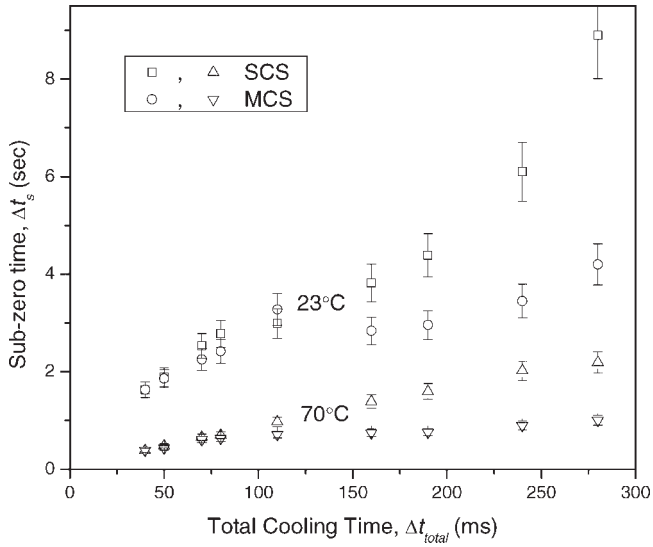

Fig. 7. Δt_s as a function of the Δt_{total}. Δt_{s} shows two different cooling regimes, in the interval $\Delta t_{\text{total}} \leq 110$ milliseconds, the differences between SCS and MCS for Δt_{s} are negligible. In the interval 110 milliseconds $< \Delta t_{\text{total}} \leq 280$ milliseconds, Δt_{s} becomes greater for SCS than for MCS by a factor of almost 2.

Figure 7 shows Δt_{s} as a function of Δt_{total} for SCS and MCS at the two T_{i}. Similar to $T_{\min}$, it is possible to distinguish two different cooling regimes. In the interval $\Delta t_{\text{total}} \leq 110$ milliseconds, the differences in Δt_{s} between SCS and MCS for each T_{i} are negligible. Δt_{s} increases linearly with Δt_{total} and the slope is greater by a factor of two for $T_{\text{i}} = 23^{\circ}\text{C}$ as compared to $T_{\text{i}} = 70^{\circ}\text{C}$. In the interval 110 milliseconds $< \Delta t_{\text{total}} \leq 280$ milliseconds, Δt_{s} is notably different between SCS and MCS for both T_{i}, and Δt_{s} becomes greater for SCS than MCS by a factor of almost 2.

Figure 8 shows Δt_{r} as a function of Δt_{total} for SCS and MCS at the two T_{i}. Similar qualitative behavior is seen for Δt_{r} compared to Δt_s (Fig. 7), except that the magnitude of Δt_{r} for experiments at $T_{\text{i}} = 70^{\circ}\text{C}$ compared to those at 23°C in the interval 110 milliseconds $< \Delta t_{\text{total}} \leq 280$ milliseconds, can be up to four times greater. The responses to the

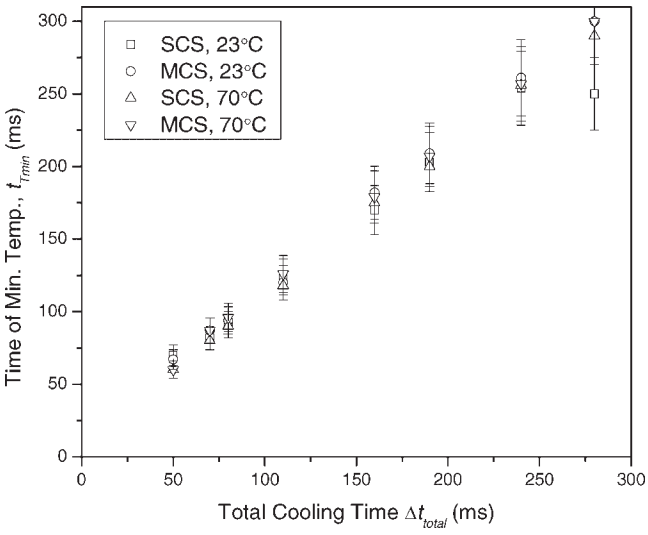

Fig. 6. Time of minimum temperature (t_{Tmin}) versus Δt_{total}, for SCS and MCS patterns at two different T_{i} temperatures (23 and 70°C). t_{Tmin} keeps the same linear increase for all cryogen spray patterns and for both T_{i}.

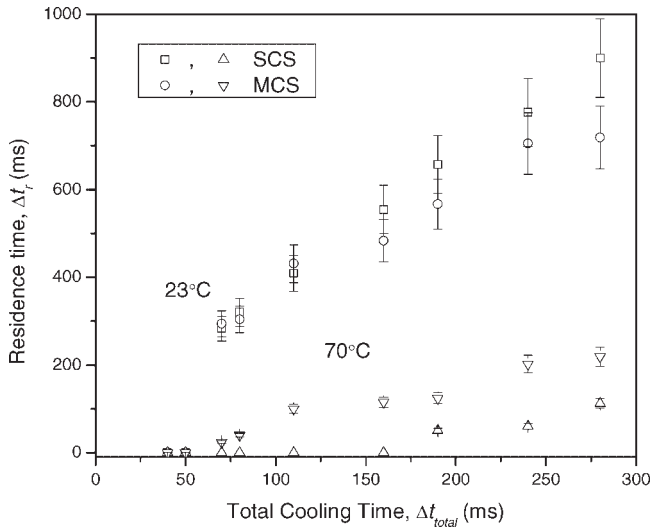

Fig. 8. Δt_{r} versus total cooling time (Δt_{total}). Note the obvious similarity between SCS and MCS, and the pronounced linear increase of Δt_{r} at $T_{\text{i}} = 23^{\circ}\text{C}$.

different spray patterns suggest that the increase in Δt_s depends on the time the surface temperature remains almost constant near T_b, as well as on the surface temperature rise from T_b to T_m (both of which may be attributed to the presence and linear evaporation of a residual cryogen layer and to the temperature gradient generated within the HSP during cryogen deposition). Longer spurts induce greater heat extraction, leading to lower HSP surface temperatures but, also, deeper cooling. The latter situation leads to lower temperature gradients close to the surface upon spurt termination and, therefore, the rate of heat transfer from the HSP to the cryogen layer is lower for longer spurts, prolonging the evaporation time, that is, Δt_s, which is clearly shown in Figure 9. Note that longer spurts lead to lower average slopes of the temperature curves in the region from T_b to T_m, as illustrated by the dotted lines. It should be noted that the temperature in this range increases ~100% faster for the shortest Δt_{total} (40 milliseconds) than for the longest (110 milliseconds). The superposition of these two linear processes leads to the linear dependency of Δt_s on Δt_{total}.

Tuqan et al. [11] recently performed histologic evaluations of in vitro model human skin exposed to four (marked with "*" in Fig. 3) of our first five MCS spray patterns. Their work demonstrated that for spurts with a Δt_{total} of 110 milliseconds or less, delivering the cryogen in MCS patterns increases the risk of cryo-injury as compared to one SCS with the same Δt_c. As such, when the Δt_{total} is less than 110 milliseconds, the risk of injury appears to depend on Δt_{total} and not Δt_c. In this study, we have shown that Δt_s continues to increase for SCS patterns while it remains essentially constant for MCS patterns within the interval 110 milliseconds $< \Delta t_{total} \leq$ 280 milliseconds, implying that for 110 milliseconds $< \Delta t_{total}$ it may be beneficial to use MCS to minimize the risk of cryo-injury to human skin during laser dermatologic surgery.

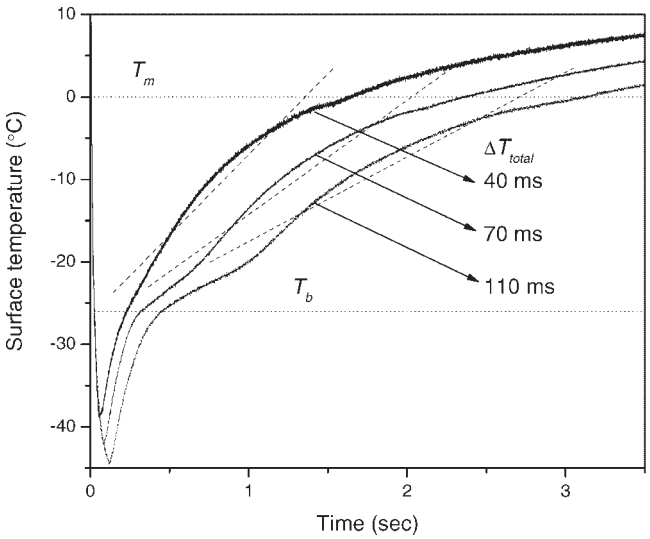

Fig. 9. Dynamic surface temperature versus time for three of the SCS studied herein with different Δt_{total}.

It is important to recognize that this HSP do not fully represent the thermal and mechanical behavior of human skin (e.g., skin indentation during CSC [19]), which might influence the magnitude of all the parameters measured in this study and, also, that our experimental procedures did not consider the combined application of cryogen and laser irradiation. Evidently, the heat generated by laser light absorption and scattering within the superficial layers of human skin would reduce both Δt_s and Δt_r. However, the present results describe the relative variation in the dynamics of the surface temperature of HSP between SCS and MCS, which is valuable information that will aid in the design of more appropriate procedures for optimal CSC on human skin.

CONCLUSIONS

An HSP was constructed and used to measure the dynamic temperature produced by MCS with the same total cryogen delivery time ($\Delta t_c = 40$ milliseconds) as SCS but with different Δt_{total}. The temporal distribution of temperature for either SCS or MCS is strongly dependent on T_i. Our results show that it is possible to distinguish between two different cooling regimes. For $\Delta t_{total} \leq$ 110 milliseconds, the differences between SCS and MCS with the same Δt_{total} are negligible for all variables under study (T_{min}, t_{Tmin}, Δt_s, Δt_r), which show a linear dependence on Δt_{total}. The longer Δt_{total}, the longer t_{Tmin}, Δt_s, Δt_r, and the lower T_{min}. This response occurs for the two T_i studied herein. In the interval 110 milliseconds $< \Delta t_{total} \leq$ 280 milliseconds, however, only Δt_s shows notable differences between SCS and MCS. For the same Δt_{total}, T_{min} is similar for SCS and MCS and Δt_s become larger for SCS than MCS by a factor of almost 2.

These results suggest that similar epidermal protection may be attained with SCS and MCS in the interval $\Delta t_{total} \leq$ 110 milliseconds. For 110 milliseconds $< \Delta t_{total} =$ 280 milliseconds, MCS help to maintain Δt_s similar to that of SCS at $\Delta t_{total} = 100$ milliseconds, which may be beneficial to prevent cryo-injury.

ACKNOWLEDGMENTS

The authors thank Daniel J. Evans and Henry Vu for computer software programming support.

REFERENCES

1. Nelson JS, Milner TE, Anvari B, Tanenbaum BS, Kimel S, Svaasand LO, Jacques SL. Dynamic epidermal cooling during pulsed laser treatment of port-wine stain. Arch Dermatol 1995;131:695–700.
2. Waldorf HA, Alster TS, McMillan K, Kauvar AN, Geronemus RG, Nelson JS. Effect of dynamic cooling on 585-nm pulsed dye laser treatment of port-wine stain birthmarks. Dermatol Surg 1997;23:657–662.
3. Chang CJ, Anvari B, Nelson JS. Cryogen spray cooling for spatially selective photocoagulation of hemangiomas: A new methodology with preliminary clinical report. Plast Reconstr Surg 1998;102:459–463.
4. Kelly KM, Nelson JS, Lask GP, Geronemus RG, Bernstein LJ. Cryogen spray cooling in combination with non-ablative laser treatment of facial rhytides. Arch Dermatol 1999;135: 691–694.

5. Nelson JS, Majaron B, Kelly KM. Active skin cooling in conjunction with laser dermatologic surgery: Methodology and clinical results. Semin Cutan Med Surg 2000;19:253–266.
6. Chang CJ, Nelson JS. Cryogen spray cooling and higher fluence pulsed dye laser treatment improve port-wine stain clearance while minimizing epidermal damage. Dermatol Surg 1999;25:767–772.
7. Aguilar G, Wang G, Nelson JS. Dynamic behavior of cryogen spray cooling: Effects of spurt duration and spray distance. Lasers Surg Med 2003;32:152–159.
8. Hirsh RJ, Farinelli WA, Anderson RR. A closer look at dynamic cooling. Lasers Surg Med 2002;(Suppl 14):36.
9. Aguilar G, Diaz SH, Lavernia EJ, Nelson JS. Cryogen spray cooling efficiency: Improvement of port wine stain laser therapy through multiple-intermittent cryogen spurts and laser pulses. Lasers Surg Med 2002;31(27):35.
10. Aguilar G, Wang G, Nelson JS. Effect of spurt duration on the heat transfer dynamics during cryogen spray cooling. Phys Med Biol 2003;48:2169–2181.
11. Tuqan AT, Kelly KM, Aguilar G, Ramirez-San-Juan JC, Sun Chung-Ho, Cassarino D, Derienzo D, Barr RJ, Nelson JS. Evaluation of tissue effects after continuous versus shorter multiple intermittent cryogen spray cooling exposure. Lasers Surg Med 2004;34:(Suppl S16):2.
12. Wang LH, Jacques SL, Zheng LQ. MCML—Monte Carlo modeling of photon transport in multi-layered tissues. Comput Methods Programs Biomed 1995;47:131–146.
13. Wang LH, Jacques SL, Zheng LQ. CONV—Convolution for response to a finite diameter photon beam incident on multi-layered tissues. Comput Methods Programs Biomed 1997;54: 141–150.
14. FEMLAB™ Reference Manual Ver 2.2. COMSOL, Inc. Burlington, MA USA: 2001.
15. Paithankar DY, Ross EV, Saleh BA, Blair MA, Graham BS. Acne treatment with a 1450 nm wavelength laser and cryogen spray cooling. Lasers Surg Med 2002;31:106–114.
16. Svaasand LO, Aguilar G, Viator JA, Randeberg LL, Kimel S, Nelson JS. Increase of dermal blood volume fraction reduces the threshold for laser-induced purpura: Implications for port wine stain laser treatment. Lasers Surg Med 2004;34:182–188.
17. Verkruysse W, Majaron B, Aguilar G, Svaasand LO, Nelson JS. Dynamics of cryogen deposition relative to heat extraction rate during cryogen spray cooling. San Jose CA: Proc SPIE 2000 3907:37–48.
18. Aguilar G, Majaron B, Verkruysse W, Nelson JS, Lavernia EJ. Characterization of cryogenic spray nozzle with application to skin cooling. In: Proceedings of the International Mechanical Engineering Congress and Exposition (IMECE). 2000. Orlando FL: FED-V. 253:189–197.
19. Basinger B, Aguilar G, Nelson JS. Effect of skin indentation on heat transfer during cryogen spray cooling. Lasers Surg and Med 2004;34:155–163.